

Flow Distribution inside an Electrostatic Precipitator: Effects of Uniform and Variable Porosity of Perforated Plate

S. M. E. HAQUE^{1*}, M. G. RASUL², M. M. K. KHAN², A. V. DEEV¹ and N. SUBASCHANDAR¹

¹Process Engineering & Light Metals (PELM) Centre
Faculty of Sciences, Engineering and Health
Central Queensland University
Gladstone, Queensland 4680
AUSTRALIA

²School of Advanced Technologies and Processes
Faculty of Sciences, Engineering and Health
Central Queensland University
Rockhampton, Queensland 4702
AUSTRALIA

Abstract: - This paper presents a numerical flow model applied to a 3D geometry of an electrostatic precipitator (ESP). The flow simulation is performed by using the computational fluid dynamics (CFD) code FLUENT. Realizable k- ϵ model for turbulence condition inside the ESP is applied. In the simulation, the perforated plates are modeled as thin porous media of finite thickness with directional permeability. Perforated plates with both uniform porosity and variable porosity are considered for simulation. The results of the simulation are discussed and compared with on-site measured data supplied by the local power plant. The simulated results show reasonable agreement with the measured data.

Key-Words: - Electrostatic precipitator; Numerical simulation; Fluent; Perforated plate; Flow distribution

1 Introduction

The performance of an ESP is significantly affected by its complex flow distribution. The flow distribution within the ESP has been reported to have varying effects on its capture performance of fly ash particles depending on the size and arrangement of an ESP. It is very difficult to carry out detailed measurements of fluid flow inside an ESP as the geometry is very complex. CFD provides an alternative method, which is viable and less expensive to study the flow behaviour inside the ESP. A suitable CFD model plays an important role in predicting the flow field characteristics and particle trajectories inside the ESP and optimizing flow distributions within the ESP by simulating proposed modification. This ensures that the required flow profiles are achieved, thus substantially reducing the outage time. However there is a limited research found in the literature for the prediction of turbulent flow behavior inside the ESP. Most of them are focused on 2D models based on simplified geometrical arrangements and ignored the role of perforated plates in uniform flow distribution inside the ESP. Zhao *et al.* [1]

predicted the effect of electro hydrodynamic flow on the main gas flow in the precipitation channel in a simple 2D model which consists of a single discharge wire and two parallel plates. The 2D model developed by Skodras *et al.* [2] consists of three wires and two parallel plates arrangements. Nikas *et al.* [3] simulated the 3D flow inside a laboratory scale precipitator of three wires and two plates arrangements. Varonos *et al.* [4] developed a 3D model and introduced smoothing grids to improve the flow characteristic of an ESP. But they simplified their model by introducing a porous region instead of creating any physical collecting plates in their CFD model. The numerical flow model of an ESP developed by Schwab and Johnson [5] replaced all the collection plates inside the ESP with equivalent resistance. Gallimberti [6] also used local loss coefficients in the governing equations to model the different wall profiles and other structures inside the ESP. Bottner and Sommerfeld [7] predicted turbulent flow in a test channel equipped with seven discharge wires. Dumont and Mudry [8] made a comparative study

on flow simulation results obtained from different precipitator CFD models.

The above studies were broadly dedicated to simulate fluid flow inside the ESP with either simplified models or simplified geometries. The aerodynamic characteristics of the flow inside an ESP in an operation may not be found without considering all of its major physical details. The present study attempts to develop a detailed numerical approach and a simulation procedure to predict the flow pattern inside an ESP of a local power station. The perforated plates of both uniform and variable porosity inside the inlet and outlet evase are taken into consideration during modeling. The predicted results are compared with the on-site measured data.

2 Geometry of ESP

The power station in this study has 4 power generating units of 350 MW capacity each. Each unit has 2 single-stage, plate-type, rigid-frame, cold-side and dry ESPs which are called as pass A and pass B. Each pass has two casing. The effective length, width and height of each casing are 30.36 m, 11 m and 13.1 m respectively. The width and height of the collection electrode (CE) walls are 5.76 m and 12.5 m respectively. Each collection wall is made of 12 collection plates. Each pass has 54 passages having 400 mm collection wall spacing. Discharge electrodes (DE) are welded into pipe frames with 2 frames per passage. The width of DE frame is 5.76m and the heights are 5 m and 7.5 m. Rapping is the dust removal method for both collection electrodes and discharge electrodes. Three perforated plates are located within the inlet evase and one outlet screen is located within the outlet evase. Due to the symmetry in geometry the numerical model is constructed to represent only one-half of a casing. Fig. 1 shows the geometrical representation of the plant ESP.

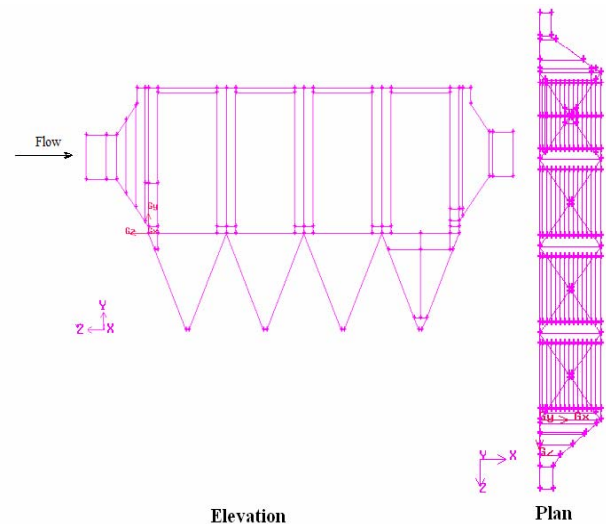


Fig.1 ESP configuration

3 Numerical Simulations

Numerical computation of fluid transport includes conservation of mass, momentum and turbulence models. "GAMBIT" is used as a preprocessor to create the geometry, discretize the fluid domain into small cells to form a volume mesh or grid and set up the appropriate boundary conditions. The flow properties are then specified and the problems are solved and analyzed by "FLUENT" solver.

The basis of modeling of an incompressible Newtonian fluid flow module is the use of the conservation of mass equation [9]

$$\frac{\partial \rho}{\partial t} + \vec{\nabla} \cdot (\rho \vec{V}) = 0 \quad (1)$$

and the momentum equation [9]

$$\frac{\partial \vec{V}}{\partial t} + \vec{V} \cdot \vec{\nabla} \vec{V} = -\frac{\vec{\nabla} p}{\rho} + \nu \vec{\nabla}^2 \vec{V} + \vec{g} \quad (2)$$

Where ρ is the fluid density and ν is the kinematic viscosity of the fluid. The pressure and velocity gradients are denoted as $\vec{\nabla} p$ and $\vec{\nabla} \vec{V}$ respectively. The realizable k- ϵ model has been used to model the turbulent flow inside the ESP [10].

A source term is added to the fluid flow equation for the pressure drop across the perforated plates. In the CFD simulation, the perforated plates

are modeled as thin porous media of finite thickness with directional permeability over which the pressure change is defined as a combination of viscous loss term and an inertial loss term which is given by

$$\Delta p = -\left(\frac{\mu}{\alpha}v + C_2 \frac{1}{2}\rho v^2\right)\Delta m \quad (3)$$

Where μ is the laminar fluid viscosity, α is the permeability of the plate, C_2 is the pressure loss coefficient per unit thickness of the plate, v is the velocity normal to the porous face and Δm is the thickness of the plate [10]. Haque *et al.* [11] found from their study that the pressure drop across the perforated plate is mainly due to the inertial loss at turbulent flow condition. The viscous loss term can be eliminated from Eq. (3) due to this reason. Appropriate values for C_2 are then calculated from the literature [12].

The finite volume methods have been used to discretize the partial differential equations of the model using the simple method for pressure-velocity coupling and the first order upwind scheme to interpolate the variables on the surface of the control volume. The segregated solution algorithm was selected. Standard wall functions were applied for near wall treatment purpose. The input parameters for the inlet were inlet velocity, turbulence intensity and hydraulic diameter. The CFD simulation was performed with a Pentium IV 1.8 GHz 32bit CPU workstation with 2GB RAM-memory and 18GB hard disc memory. Fig. 2 shows the model ESP developed in GAMBIT.

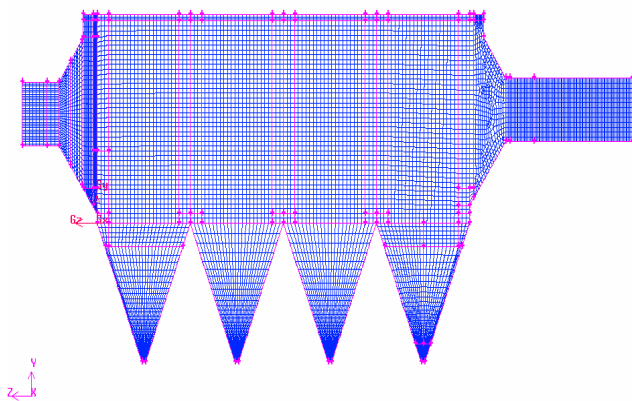


Fig. 2: Numerical grid for ESP

4 Results and Discussions

4.1 Onsite Measurement

A windmill vane type anemometer was used to measure the velocity at different planes inside the ESP casings. Measurements were taken by Dattner and Donaldson [13] at plane 2, 3 and 4 as shown in Fig. 3 with the unit offline and the ID fans operating. Measurement of the velocity inside the ESP was carried out for the average inlet velocity of 9.36 m/s at an average temperature of 24^o C. Table 1 shows measured velocity distribution at three planes inside the ESP at height 11.8 m.

Table 1: Velocity distribution inside the ESP

Centre to wall distance (m)	Velocity (m/s)		
	Plane 1	Plane 2	Plane 3
0.5	1.01	1.13	1.01
1.5	1.11	1.19	0.95
2.5	1.21	1.13	1.08
3.5	1.31	1.13	0.95
4.5	0.81	1.13	1.01

4.2 CFD Prediction and Data Comparison

The inlet boundary condition of the CFD model of the ESP was set as a “velocity-inlet” with a value of 9.36 m/s. The outlet boundary condition was set as a “pressure-outlet”.

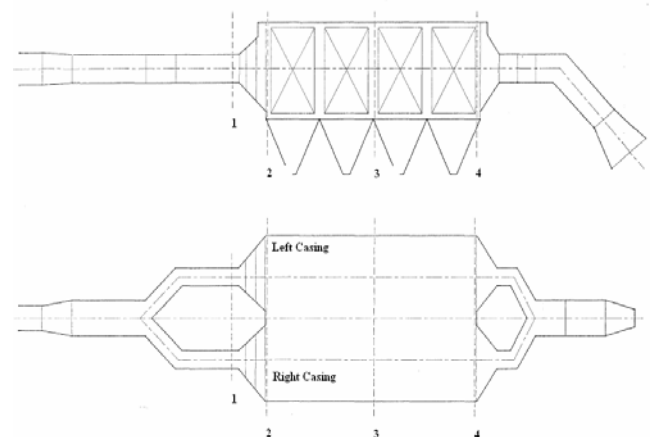


Fig. 3: Measurement planes for velocity distribution

Two simulations have been carried out for both uniform and variable porosity of perforated plate. The simulated results obtained by considering uniform porosity of perforated plate are presented in Figs. 4 and 5 where velocity distributions are found non-uniform. The predicted velocity at height $y=11.8$ m of plane 2, 3 and 4 as shown in

Fig. 3 are compared with the measured velocity. Figs. 6, 7 and 8 present the velocity comparison at three measurement planes, which give a reasonably good prediction with a maximum deviation of about 20% on the measured values. Figs. 9 and 10 present the velocity profiles after introducing the variable porosity of perforated plate in the model. The results show that the flow is more uniformly distributed now. The predicted velocity at plane 2 is then compared with the available on-site data which is shown in Fig. 11. The prediction is found satisfactory with minor deviation from the measured data. The deviation which is acceptable to the power plant may be due to the influence of flow angularity [7].

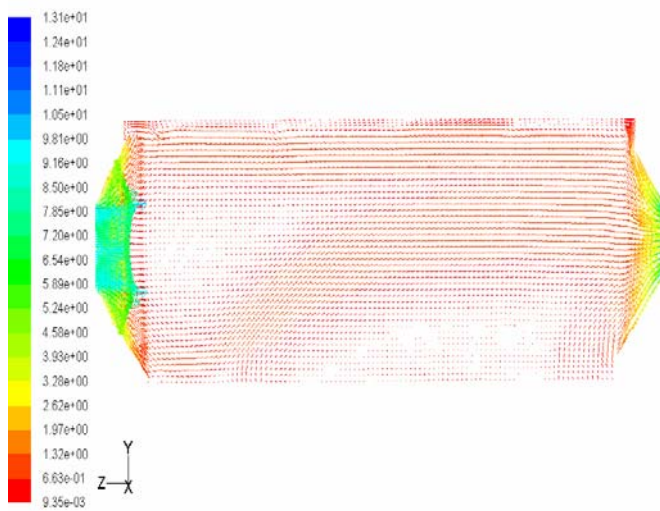


Fig. 4: Velocity distribution at x=0 m (symmetry plane – side view) considering uniform porosity of perforated plate

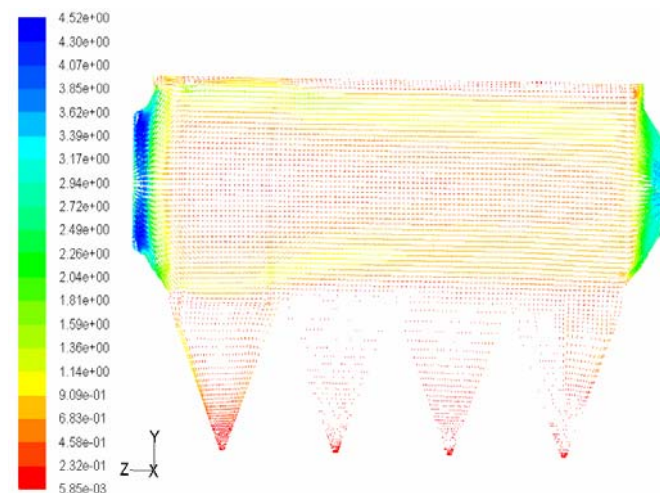


Fig. 5: Velocity distribution at x=2.75 m (side view) considering uniform porosity of perforated plate

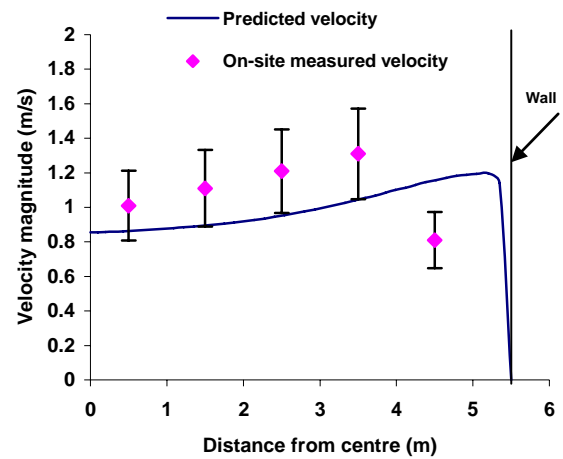


Fig. 6: Velocity magnitude at y=11.8 m (Plane 2). Comparison between prediction and measurement

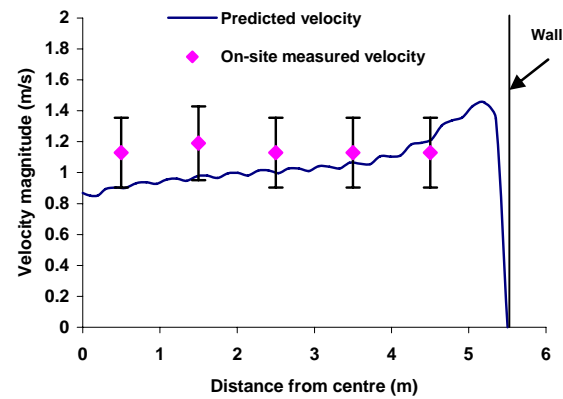


Fig. 7: Velocity magnitude at y=11.8 m (Plane 3). Comparison between prediction and measurement

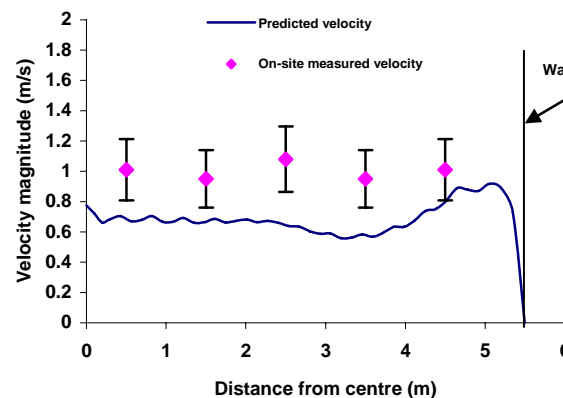


Fig. 8: Velocity magnitude at y=11.8 m (Plane 4). Comparison between prediction and measurement

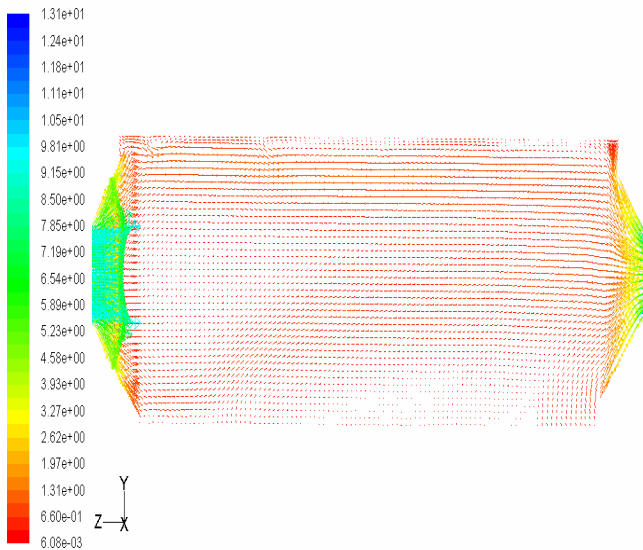


Fig. 9: Velocity distribution at x=0 m (symmetry plane - side view) considering variable porosity of perforated plate

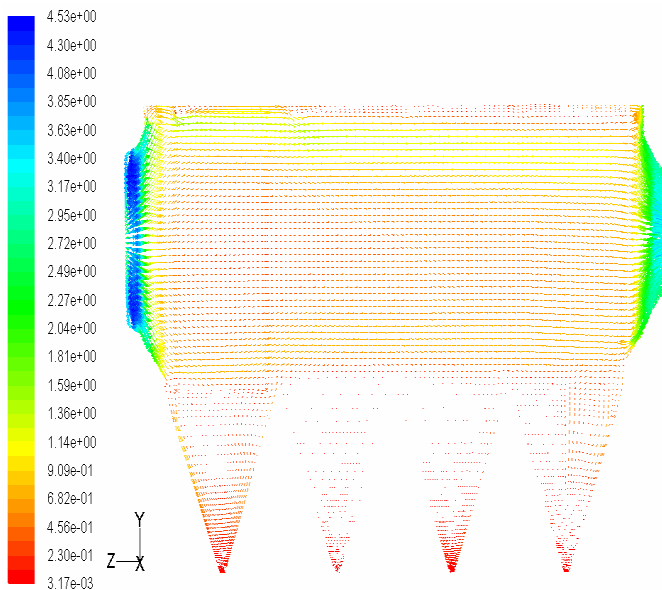


Fig.10: Velocity distribution at x=2.75 m (side view) considering variable porosity of perforated plate

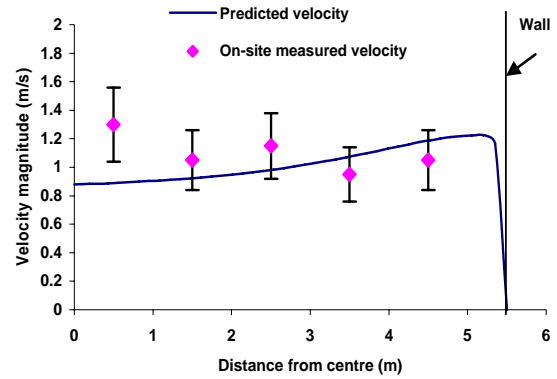


Fig. 11: Velocity magnitude at y=11.8 m (Plane 2). Comparison between prediction and measurement considering variable porosity of perforated plate

5 Concluding Remarks

A CFD analysis for an ESP of a local power plant is presented. The perforated plates are modeled as thin porous surface with directional permeability. The effect of using variable porosity of perforated plate on the improvement of flow distribution inside the ESP is discussed. The study shows that the variable porosity of perforated plate is effective to achieve uniform flow distribution inside the ESP. Study of such three dimensional flow gives a good prediction on the effects of flow distribution on the particle residence time inside the ESP. This model can be useful in identifying options on operation and maintenance improvement activities by ESP tuning, optimizing flow distribution, field charging and rapping cycles and necessary plant modifications.

Acknowledgements

The authors would like to thank Stanwell Corporation Limited for supporting this work and providing on-site measured data.

References:

- [1] L. Zhao, E. Dela Cruz, K. Adamiak, A.A. Berezin, J.S. Chang, A numerical model of a wire-plate electrostatic precipitator under electrohydrodynamic flow conditions, Conference proceedings. The 10th International conference on electrostatic precipitator, Australia, 2006.
- [2] G. Skodras, S.P. Kaldis, D. Sofialidis, O. Faltsi, P. Grammelis, G.P. Sakellaropoulos, Particulate removal via electrostatic

- precipitators – CFD simulation, *Fuel Processing Technology*, Vol. 87, 2006, pp 623 – 631.
- [3] K.S.P.Nikas, A.A.Varnos, G.C.Bergeles, Numerical simulation of the flow and the collection mechanisms inside a laboratory scale electrostatic precipitator, *Journal of Electrostatics*, Vol. 63, 2005, pp 423-443
- [4] A.A.Varonos, J.S.Anagnostopoulos, G.C.Bergeles, Prediction of the cleaning efficiency of an electrostatic precipitator, *Journal of Electrostatics*, Vol. 55, 2002, pp. 111 – 133
- [5] M. J. Schwab, R. W. Johnson, Numerical design method for improving gas distribution within electrostatic precipitators, *Proceedings of the American Power Conference*, Vol. 56, 1994, pp. 882-888
- [6] I. Gallimberti, Recent advancements in the physical modeling of electrostatic precipitators. *Journal of electrostatics*, Vol. 43, 1998, pp 219- 247.
- [7] C.U.Bottner, M.Sommerfeld, Euler/Lagrange calculations of particle motion in turbulent flow coupled with an electric field, *Proceedings of ECCOMAS Computational Fluid Dynamics Conference*, 2001
- [8] B.J.Dumont, R.G.Mudry, Computational fluid dynamic modeling of electrostatic precipitators, *Proceedings of Electric power 2003 conference*, 2003
- [9] B.R.Munson, D.F.Young, T.H.Okiishi, *Fundamentals of fluid mechanics*, 4th ed., John Wiley & Sons Inc., NY, 2002
- [10] *Fluent 6.2 User's Guide*, Fluent Inc., 2005
- [11] S. M. E. Haque, M. G. Rasul, A. Deev, M. M. K. Khan, J. Zhou, The influence of flow distribution on the performance improvement of electrostatic precipitator, *Proceedings, International Conference on Air Pollution Abatement Technologies-Future Challenges*, Australia, 2006
- [12] I. E. Idelchik, *Handbook of hydraulic resistance*, 3rd edition, CRC Press Inc., 1994
- [13] R. Dattner, I. Donaldson, Gas distribution measurement report, Stanwell Power Station, 1992.